More Fault Connectivity Is Needed in Seismic Hazard Analysis

Morgan T. Page*[1]

ABSTRACT

Did the third Uniform California Earthquake Rupture Forecast (UCERF3) go overboard with multifault ruptures? Schwartz (2018) argues that there are too many long ruptures in the model. Here, I address his concern and show that the UCERF3 rupture-length distribution matches empirical data. I also present evidence that, if anything, the UCERF3 model could be improved by adding more connectivity to the fault system. Adding more connectivity would improve model misfits with data, particularly with paleoseismic data on the southern San Andreas fault; make the model less characteristic on the faults; potentially improve aftershock forecasts; and reduce model sensitivity to inadequacies and unknowns in the modeled fault system.

KEY POINTS

- The UCERF3 model has a rupture-length distribution that matches empirical data.
- Adding more connectivity to UCERF3 would improve data misfits.
- More connectivity in seismic hazard models would make them less sensitive to fault model uncertainties.

Supplemental Material

INTRODUCTION

The third Uniform California Earthquake Rupture Forecast (UCERF3; Field *et al.*, 2014) is novel in several ways. It is derivative rather than prescriptive, with an inversion to solve for rupture rates instead of expert-opinion voting (Page *et al.*, 2014). It bridges the medium-term forecasting gap (Jordan, 2012) by linking a long-term, fault-based earthquake rupture forecast, complete with elastic rebound effects (Field *et al.*, 2015), with short-term clustering driven by aftershock triggering (Field *et al.*, 2017). Finally, it is one of the first seismic hazard models to include multifault ruptures. All of these changes required methodological innovation; the end result is a model that is much more sophisticated than previous hazard models in California.

In this article, I focus on the introduction of multifault ruptures into the UCERF3 model, which substantially increased the connectivity of the fault system. The inclusion of multifault ruptures has opened up the model to criticism, most notably by Schwartz (2018), who argues that the model has too many long ruptures. I show that, in fact, UCERF3 matches the observed rupture-length distribution—that is, the fraction of earthquakes with a given rupture length—quite well, and better than previous models.

Furthermore, I argue that not only was the inclusion of multifault ruptures an improvement on past practice, as it allows the model to include ruptures much like those that have been observed in the past, but also that there is still further progress that can be made in this direction. Further increasing connectivity in hazard models such as UCERF will reduce model misfits, as well as make the model less sensitive to inadequacies in the fault model and provide a better approximation of the natural system.

RUPTURE-LENGTH DISTRIBUTION

In a recent article, Schwartz (2018) criticizes the UCERF3 model and suggests that it has too many long ruptures (i.e., those with rupture lengths ≥100 km). He mistakenly compares the observed rupture-length distribution (a dataset of 258 historical surface ruptures from Wells and Youngs, 2013) with the discretization of ruptures in the UCERF3 model. This comparison is inaccurate and inappropriate because it does not take into account the rate at which ruptures of a given length actually occur in UCERF3. (The discretization of the model is irrelevant for comparison to data. For example, all large ruptures could be discretized twice as finely as they are currently, resulting in twice as many large ruptures; however, the rate of each would halve, and the resulting hazard would be the same.) In Figure 1, I show the appropriate comparison between the observed rupture-length distribution of Wells and Youngs (2013) and the rupture-length distribution for UCERF3 "on-fault" earthquakes (these are earthquakes that occur on

1. U.S. Geological Survey, Pasadena, California, U.S.A.

*Corresponding author: pagem@caltech.edu

Cite this article as Page, M. T. (2020). More Fault Connectivity Is Needed in Seismic Hazard Analysis, *Bull. Seismol. Soc. Am.* **XX**, 1–7, doi: 10.1785/0120200119

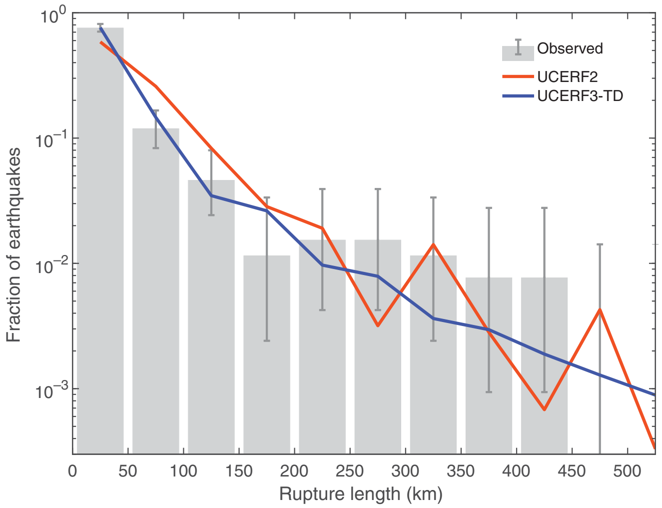

Figure 1. Observed historical rupture lengths (Wells and Youngs, 2013) compared with rupture lengths from Uniform California Earthquake Rupture Forecast, version 2 (UCERF2) and the mean long-term time-dependent third Uniform California Earthquake Rupture Forecast (UCERF3-TD) model. Error bars show 95% confidence bounds on the true underlying rupture length proportions, assuming that the 258 observed rupture lengths are independent observations of the underlying rupture-length distribution. Note that UCERF3 lies within the 95% confidence bounds derived from the observed rupture lengths, whereas UCERF2 does not.

the modeled faults in UCERF3, which have a rupture length equal to or exceeding the seismogenic fault width). This is the appropriate comparison to make because it shows, for each synthetic or observed dataset, the fraction of earthquakes that actually occur with a given rupture length. The UCERF2 model (Field *et al.*, 2007) is also shown for comparison. As Figure 1 shows, the mean long-term time-dependent UCERF3 (UCERF3-TD) model (Field *et al.*, 2015) falls within the 95% confidence bounds derived from the observed rates, whereas the previous model, UCERF2, does not match the observations at 95% confidence for half of the bins. To have a large dataset for comparison, this figure uses the entire global dataset of Wells and Youngs (2013). California earthquakes make up 12% of this dataset, and a Kolmogorov–Smirnov test shows that the California earthquakes do not have a significantly different rupture-length distribution than the entire dataset ($p = 0.34$). Indeed, the California earthquake subset (Fig. S1, available in the supplemental material to this article) shows a similar pattern as Figure 1, albeit with fewer observed data for comparison. Figure S1 also shows that, as with the global dataset, UCERF3 matches observed California data better than UCERF2.

There is some hint in Figure 1 that, if anything, the UCERF3 model might underpredict the rates of ruptures over 200 km in length, given that the model underpredicts the data (but is within the uncertainties) for bins from 200 to 400 km of rupture length. This is consistent with comparisons to the Wesnousky database of surface ruptures (Wesnousky, 2008): compared with this dataset, the UCERF3 model has fewer multifault ruptures and fewer ruptures with jumps >1 km (Page *et al.*, 2014).

Finally, 0.47% (not 32%, as claimed by Schwartz, 2018) of UCERF3 surface-rupturing earthquakes, by rate, are >500 km. This is not inconsistent with the lack of observed ruptures >500 km in the observed dataset of only 258 ruptures (Wells and Youngs, 2013).

CONNECTIVITY: DOES UCERF3 GO FAR ENOUGH?

Incorporating multifault ruptures was a goal of the UCERF3 project, in part because they could alleviate discrepancies in the model, such as the problem of the "bulge," that is, an overprediction in the rate of M_w 6.5–7 earthquakes. Multifault ruptures were also included in UCERF3, certainly, because they are routinely observed, as in the famous examples of the 1992 M_w 7.3 Landers, California (Sieh *et al.*, 1993) and 2002 M_w 7.9 Denali, Alaska (Eberhart-Phillips *et al.*, 2003) earthquakes. Following the publication of the model, the UCERF3 approach was vindicated by research suggesting that the Newport–Inglewood and Rose Canyon faults can rupture together (Sahakian *et al.*, 2017), which is allowed in UCERF3, and by the poster child of multifault ruptures, the 2016 M_w 7.8 Kaikōura, New Zealand, earthquake, which ruptured >20 mostly distinct faults (Litchfield *et al.*, 2018). Integration of techniques from multiple fields such as light detection and ranging (LiDAR), Interferometric Synthetic Aperture Radar (InSAR), and geological field mapping allowed the complex Kaikōura rupture to be imaged in such detail. This suggests that the seeming tendency for more observed complexity in recent earthquakes (e.g., the 2010 El Mayor–Cucapah and 2012 M_w 8.6 Sumatra earthquakes) is due to improved data, which allows for better resolution of fault rupture, rather than coincidence. This improved resolution of rupture complexity, combined with seismological evidence that the size distribution and triggering potential are insensitive to proximity to major faults (Page and van der Elst, 2018), suggests that individual earthquakes may have the same (fractal) complexity as the fault network itself.

If this is the case, how can we hope to capture the full plethora of earthquakes that may occur in seismic hazard models? Following the Kaikōura earthquake, the natural impulse is to ask if the UCERF3 methodology, applied to the New Zealand fault system, would have included for the possibility of this earthquake. The answer, in the literal sense, is almost certainly no. Even leaving aside the problem that not all faults that ruptured were presumed active prior to the earthquake (Litchfield *et al.*, 2018), the UCERF3 rupture set does not include every possible set of faults that can feasibly rupture together, for reasons of both computational tractability and scientific improbability (Milner *et al.*, 2013). For example, modeled ruptures were not allowed to jump more than 5 km between different faults. This binary rule (ruptures are either included in the

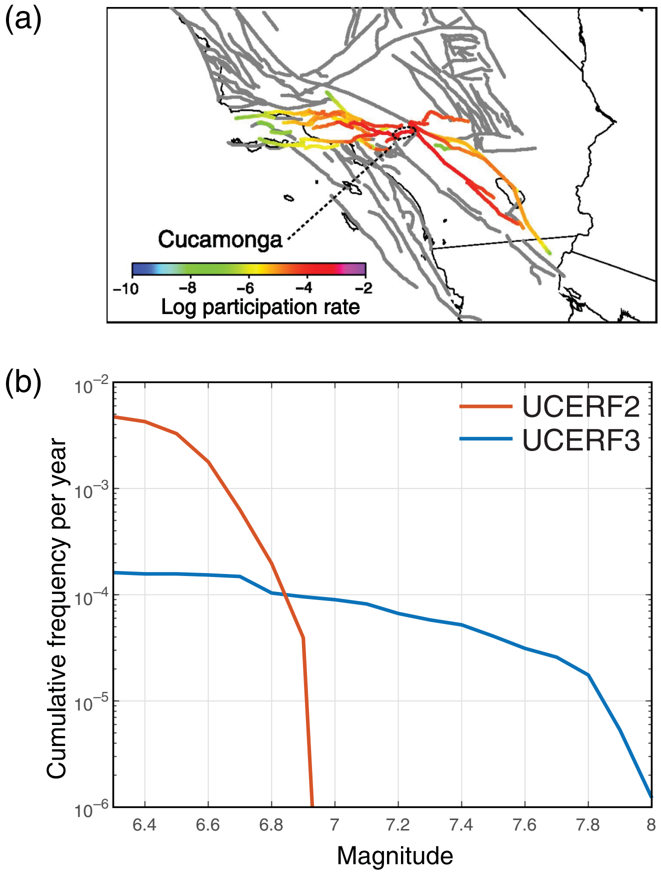

Figure 2. Fault connectivity controls the local magnitude distribution and maximum magnitude in UCERF models. (a) Faults that participate in multifault ruptures with the Cucamonga fault in UCERF3, colored by yearly rate. (b) Magnitude (M_w) distributions for earthquakes nucleating on the Cucamonga fault in UCERF2 and UCERF3. In the UCERF2 model, the Cucamonga fault does not rupture with other faults.

rupture set or not) is consistent with the ruptures in the Wesnousky dataset of fault surface ruptures (Wesnousky, 2008). However, it was known at the time of the UCERF3 development to, at least occasionally, be violated, as it was in the 2010 El Mayor–Cucapah earthquake, which had a jump between faults of ∼11 km (Fletcher *et al.*, 2016). (However, this large of a jump is allowed in the UCERF3 epidemic type aftershock sequence [UCERF3-ETAS] model as a separate, triggered event.) To give a second example, the cumulative azimuth filter in UCERF3 (known colloquially as the "squirrelly-ness" filter), which removes ruptures for which the cumulative azimuth changes along strike exceed a given threshold, was developed solely to keep the number of ruptures in the model computationally tractable. Without this filter, possible rupture combinations traversing the high density of faults in the Ventura and Los Angeles basins would have numbered in the hundreds of millions.

To obtain the correct mean hazard, however, it is not necessary for UCERF3 to predict the exact rupture process likely to happen in a future Kaikōura-like rupture. What is necessary, however, is for the model to capture enough connectivity so that the modeled magnitude distribution—including the maximum magnitude—is accurate. Connectivity in the UCERF3 model controls the magnitude distribution on modeled faults because it determines the maximum allowed magnitude. This is illustrated in Figure 2, which compares moment magnitude distributions for the Cucamonga fault in UCERF2 and UCERF3. In the UCERF2 model, this fault was modeled as rupturing independently—it was not allowed to "link up" with neighboring faults to form $M_w \geq 7$ ruptures. In UCERF3, it could link up with nearby faults in a number of different ways, as shown in Figure 2a, in which faults are colored by the rate in which they participate in ruptures with the Cucamonga fault. Both the UCERF2 and UCERF3 models are slip rate balanced, but the UCERF2 model requires a much higher rate of moderate ($M_w \approx 6.5$) earthquakes to match the Cucamonga fault's slip rate, given that larger magnitude earthquakes are not allowed in UCERF2. By contrast, in the UCERF3 model, much of the moment on this fault can be apportioned to $M_w \geq 7$ earthquakes, which results in lower earthquake rates (and lower hazard, incidentally) on the Cucamonga fault.

Although the UCERF3 model does have more fault connectivity than UCERF2, there are still faults in UCERF3 with quite low maximum magnitudes due to low connectivity. One extreme example of this in the UCERF3 model is the 17-km-long Robinson Creek fault in the eastern Sierra, which does not connect with any other modeled faults because it is >5 km away from them. Because of the lack of connectivity with neighboring faults, the maximum magnitude on this fault is modeled to be 6.5. This is lower than the maximum magnitude allowed for off-fault seismicity, which, depending on the logic-tree branch, is either 7.2, 7.6, or 8.0. Thus, in this area, and indeed, throughout northeastern California (see Fig. 3) it is assumed, paradoxically, that earthquakes on the known faults cannot be as large as those on unknown faults.

Faults such as the Robinson Creek fault are obvious starting points for adding more connectivity to the model. Adding connectivity also makes faults, on average, less characteristic. In the case of the Robinson Creek fault, it has a relatively low seismicity rate, based on observed seismicity near the fault, compared with its average UCERF3 target slip rate of 0.6 mm/yr. As a result, the Robinson Creek fault is the most characteristic fault in the UCERF3 model, meaning, for this fault, the rate of large earthquakes far surpasses a Gutenberg–Richter extrapolation from the small-earthquake rate. In fact, for this fault, the minimum supraseismogenic magnitude (i.e., the magnitude for which the rupture is as long as the seismogenic width of the fault) rate is 72 times higher than that the small-earthquake rate would predict with a Gutenberg–Richter extrapolation.

Adding more connectivity to UCERF3 would also help better match the underlying data in the model. For example,

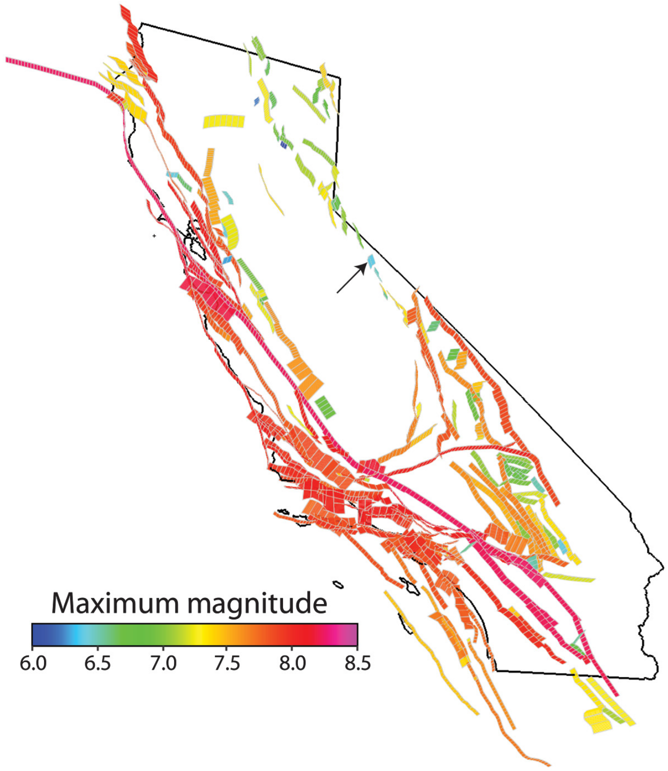

Figure 3. Maximum magnitude (M_w) for faults in UCERF3 is highly spatially variable and is determined by fault connectivity assumptions. The small black arrow identifies the Robinson Creek fault, a poorly connected fault discussed in the Connectivity: Does UCERF3 Go Far Enough? section.

paleoevent rates along the southern San Andreas fault were systematically underestimated in UCERF3 (at each paleosite along the southern San Andreas, the model rate underpredicted the mean observed rate, but was within the 95% confidence bound) (Page *et al.*, 2014). As with all inverse problems with global constraints, misfits or incorrect model parameterizations in one area of the model can affect other areas. In the UCERF3 model, the total number of earthquakes is limited globally to match long-term seismicity rates inferred from historical seismicity and seismicity variability (Felzer, 2013). In this case, if the finite supply of moderate-sized earthquakes is used up to match slip rates on poorly connected faults elsewhere in California, there may not be enough of these earthquakes to match the high paleoseismic rates on fast-moving faults such as the San Andreas. Increasing connectivity along some faults could allow more freedom for the inversion to match paleoseismic rates on other faults.

Within the UCERF3 logic tree, data misfits vary dramatically depending on the logic-tree branch. These misfits can potentially illuminate fundamental inconsistencies in the data, the model parameterization, or both. In general, better-fitting branches allow more slip in large earthquakes (e.g., the Hanks and Bakun, 2002 scaling relation) or more total earthquakes. Although individual branches have total moment rates ranging from 79% to 115% of the total on-fault target moment, most branches underpredict the target moment, and mean UCERF3 underpredicts the target moment rate by 1%. The slip rates in the model are difficult to match without allowing either more earthquakes or more slip in the largest earthquakes. Increasing connectivity within the model would therefore also improve misfits because this would allow more slip on faults to be apportioned to large, rather than small, earthquakes.

Finally, UCERF3 slip-rate fits along the creeping section of the San Andreas provide more evidence that increased connectivity would improve data misfits. In UCERF3, creep rates are modeled to have a "rainbow" shape along the creeping section, with the highest rates of creep in the center (Titus *et al.*, 2006; Tong *et al.*, 2013). In previous hazard models in California, earthquakes connecting the southern and northern parts of the San Andreas were not allowed. The philosophy in UCERF3 was somewhat different—although historical earthquakes have not ruptured through the creeping section, such an event could be possible but rare. To include a small but nonzero probability of a throughgoing rupture, at the center of the creeping section, in addition to a reduction in the seismogenic area, the target slip rate is reduced by 80% to account for the portion of creep at depth (Page *et al.*, 2013). This slip-rate reduction limits the rate of throughgoing ruptures connecting the northern and southern San Andreas; if the target slip rate in the center of the creeping section were matched by the model, throughgoing ruptures would be reduced by a factor of 5 compared with a model in which the creeping section was fully locked. However, the inversion solution in UCERF3 does not match the target slip rate at the center of the creeping section; in fact, the model slip rate on that portion of the fault is twice the target. Although the creeping section is still somewhat of a barrier to throughgoing ruptures, it is not as much of a barrier as it would be if the slip rate were better matched here, which would be possible if connectivity elsewhere were increased. Tellingly, in this unique area of the UCERF3 model in which increased connectivity is not explicitly prohibited by model parameterization, the solution has more connectivity than the data inputs would imply. This connectivity in the solution is added by overpredicting the target slip rate at the center of the creeping section, which is preferred, in terms of global misfits, given the other data being fit by the inversion within the parameterization of the model.

CONNECTIVITY AND CHARACTERISTIC-NESS

How much of an effect on the final model would increasing connectivity have? One measure of this is the "characteristic-ness," relative to a Gutenberg–Richter magnitude distribution, of the on-fault portion of UCERF3. On average, the faults in UCERF3 have a characteristic magnitude distribution, although the off-fault portion of the model is anticharacteristic, so that the total model, with on-fault and off-fault seismicity together, matches a Gutenberg–Richter magnitude distribution. The characteristic-ness of the on-fault seismicity in UCERF3 varies by logic-tree branch (namely, it is affected by the choice of magnitude–area scaling relation, the deformation model, and the total seismicity rate). For example, with the reference deformation model (Zeng and Shen, 2014), Hanks and Bakun (2002) magnitude scaling, and the reference branch for total seismicity rate (the median rate of 7.9 $M_w \geq 5$ earthquakes per year), total on-fault moment would have to be reduced by 33% to make the model Gutenberg–Richter for both on-fault and off-fault components. This rather large reduction, which is a measure of the model characteristic-ness, is due to the fact that the fraction of seismic moment on modeled faults in the UCERF3 model is greater than the fraction of seismicity on modeled faults. If connectivity in UCERF3 were improved so that all modeled faults could participate in earthquakes up to magnitude 8 (still not as large as the largest on-fault earthquake in the model but comparable with the largest off-fault maximum magnitude assumed), this branch would instead require a 22% moment-rate reduction on faults for the on-fault moment fraction to equal the on-fault seismicity fraction (which is what a Gutenberg–Richter model would require). This statistic gives a sense of how much connectivity could potentially change the moment distribution of the model, given that many of the poorly connected faults in UCERF3 have fairly low slip rates. Without making further changes to UCERF3, this branch of UCERF3 is not compatible with on-fault Gutenberg–Richter magnitude scaling without a substantial on-fault moment reduction. If we instead consider this same branch but with a higher total seismicity rate (e.g., the highest seismicity-rate branch of 9.6 $M_w \geq 5$ earthquakes per year), increasing connectivity to magnitude 8 for all faults in the system does make a Gutenberg–Richter model possible without additional on-fault moment rate reductions.

Therefore, although increasing connectivity alone is not enough, for most branches, to remove the "characteristic-ness" of the on-fault portion of UCERF3, it will, in general, make the model less characteristic on the faults. Whether faults are characteristic is still a matter of debate, with evidence on both sides (e.g., Hecker *et al.*, 2013; Page and Felzer, 2015). However, making faults less characteristic could be advantageous, given that some faults in the long-term model are more characteristic than empirical aftershock productivity relations imply, meaning that a large earthquake on those faults would produce more small aftershocks than the modeled magnitude distribution on the fault assumes. This currently means that UCERF3-ETAS, the version of UCERF3 that includes short-term clustering from aftershock triggering, is not entirely consistent with the long-term model. Furthermore, in general, the magnitude distributions on faults affect aftershock productivity in a way that, although consistent with the hypothesis of characteristic magnitude distributions, has not been directly observed (Michael, 2012). This was evident in UCERF3-ETAS forecasts for the 2019 Ridgecrest sequence (Milner *et al.*, 2020). Aftershock probabilities produced by the full version of the model for this sequence were lower than those produced by a no-faults version of the model. The reason for the difference in aftershock probabilities between the full version of UCERF3-ETAS and no-faults UCERF3-ETAS is due to the difference in local magnitude distributions; namely, the no-faults version of the model has Gutenberg–Richter scaling everywhere. This example highlights the importance of getting any characteristic behavior correct, given its effect on aftershock statistics. Increasing fault connectivity in UCERF3, particularly making connectivity more spatially uniform, would result in a model less sensitive to areas where the fault mapping may be poor, which influences local magnitude distributions in the model. Making connectivity more spatially uniform is also a more conservative choice, allowing the model to produce more spatially uniform aftershock productivities without throwing out valuable information about well-located faults.

CONCLUSIONS

I have shown that adding multifault ruptures to UCERF3 improved fits to empirical rupture-length data but that some areas of the model still have poor connectivity, which affects model misfits and local magnitude distributions. Improving connectivity would make the model less characteristic, more spatially uniform, and less sensitive to fault model unknowns.

Future versions of UCERF can certainly improve upon the simple fault-linking rules of Milner *et al.* (2013); as discussed previously, the 5-km rule for allowing faults to link has been broken in previous earthquakes. Paleoseismic and geologic constraints can hopefully better tune which ruptures are possible and probable. In addition, physics-based rupture modeling can be used to generate much longer histories than the paleoseismic record and generate statistics of probable rupture scenarios. In particular, the physics-based simulator RSQSim (Richards-Dinger and Dieterich, 2012), when applied to the UCERF3 fault system, produces less spatial variation in dominant magnitude (defined as the median of the moment distribution) than the UCERF3 model (Shaw *et al.*, 2018). This is because in the RSQSim model, fault connectivity is not prescribed; rather, it emerges from quasidynamic simulations of fault behavior. Notably, RSQSim catalogs contain higher dominant magnitudes on secondary faults, including faults in northeastern California that are poorly connected in UCERF3. Major faults that are well-connected in UCERF3 have lower dominant magnitudes in RSQSim catalogs. By this measure, the physics-based simulator approach thus yields more spatially uniform magnitude distributions and more uniform connectivity than UCERF3.

The more fundamental problem within UCERF3, which underlies the connectivity issues, is the false dichotomy between "on-fault" and "off-fault" (background) earthquakes. Earthquake simulators such as RSQSim have a similar separation. Yet statistical evidence does not support a difference between earthquakes, in terms of productivity or size scaling, among earthquakes along major, high-slip-rate faults, and earthquakes in the "bulk" (Page and van der Elst, 2018). Given that nature cannot tell the difference between the "on-fault" and "off-fault" regime (after all, all earthquakes occur on faults), we should design our models with a similar nondistinction. In the simplest version of such a model, we could allow ruptures to propagate beyond the mapped ends of known faults. A more complex model would allow stochastic faults, different with each model realization, to link known faults in kinematically sensible ways. Such a solution could make use of the off-fault strain field, not currently used in the UCERF3 model, to place possible unmapped faults.

DATA AND RESOURCES

The third Uniform California Earthquake Rupture Forecast (UCERF3) code is available at https://github.com/OpenSHA (last accessed March 2020). An additional figure comparing the observed length distribution for surface-rupturing earthquakes in California with UCERF2 and UCERF3 is available in the supplemental material to this article.

ACKNOWLEDGMENTS

The author thanks Kevin Milner for pulling information from the third Uniform California Earthquake Rupture Forecast (UCERF3) code behemoth. The author also acknowledges helpful reviews from Ned Field, Alex Hatem, Suzanne Hecker, Andy Nicol, and Rich Koehler.

REFERENCES

Eberhart-Phillips, D., P. J. Haeussler, J. T. Freymueller, A. D. Frankel, C. M. Rubin, P. Craw, N. A. Ratchkovski, G. Anderson, G. A. Carver, A. J. Crone, *et al.* (2003). The 2002 Denali fault earthquake, Alaska: A large magnitude, slip-partitioned event, *Science* **300,** no. 5622, 1113–1118.

Felzer, K. R. (2013). Appendix L—Estimate of the seismicity rate and magnitude-frequency distribution of earthquakes in California from 1850 to 2011, Uniform California Earthquake Rupture Forecast, version 3 (UCERF3), *U.S. Geol. Surv. Open-File Rept. 1165*, 13 pp.

Field, E. H., R. J. Arrowsmith, G. P. Biasi, P. Bird, T. E. Dawson, K. R. Felzer, D. D. Jackson, K. M. Johnson, T. H. Jordan, C. Madden, *et al.* (2014). Uniform California Earthquake Rupture Forecast, version 3 (UCERF3)—The time-independent model, *Bull. Seismol. Soc. Am.* **104,** no. 3, 1122–1180.

Field, E. H., G. P. Biasi, P. Bird, T. E. Dawson, K. R. Felzer, D. D. Jackson, K. M. Johnson, T. H. Jordan, C. Madden, A. J. Michael, *et al.* (2015). Long-term time-dependent probabilities for the third Uniform California Earthquake Rupture Forecast (UCERF3), *Bull. Seismol. Soc. Am.* **105**, no. 2A, 511–543.

Field, E. H., T. E. Dawson, K. R. Felzer, A. D. Frankel, V. Gupta, T. H. Jordan, T. Parsons, M. D. Petersen, R. S. Stein, R. J. Weldon II, *et al.* (2007). The Uniform California Earthquake Rupture Forecast, version 2 (UCERF2), *U.S. Geol. Surv. Open-File Rept. 2007-1437*, 104 pp.

Field, E. H., K. R. Milner, J. L. Hardebeck, M. T. Page, N. van der Elst, T. H. Jordan, A. J. Michael, B. E. Shaw, and M. J. Werner (2017). A spatiotemporal clustering model for the third Uniform California Earthquake Rupture Forecast (UCERF3-ETAS): Toward an operational earthquake forecast, *Bull. Seismol. Soc. Am.* **107,** no. 3, 1049–1081.

Fletcher, J., M. Oskin, and O. Teran (2016). The role of a keystone fault in triggering the complex El Mayor–Cucapah earthquake rupture, *Nature Geosci.* **9,** 303–307.

Hanks, T. C., and W. H. Bakun (2002). A bilinear source-scaling model for M–log *A* observations of continental earthquakes, *Bull. Seismol. Soc. Am.* **92,** no. 5, 1841–1846.

Hecker, S., N. A. Abrahamson, and K. E. Wooddell (2013). Variability of displacement at a point: Implications for earthquake-size distribution and rupture hazard on faults, *Bull. Seismol. Soc. Am.* **103,** no. 2A, 651–674.

Jordan, T. H. (2012). Earthquake forecasting as a system-science problem, *AGU Fall Meeting Abstracts*, available at https://abstractsearch.agu.org/meetings/2012/FM/S23C-01.html (last accessed October 2020).

Litchfield, N. J., P. Villamor, R. J. V. Dissen, A. Nicol, P. M. Barnes, D. J. A. Barrell, J. R. Pettinga, R. M. Langridge, T. A. Little, J. J. Mountjoy, *et al.* (2018). Surface rupture of multiple crustal faults in the 2016 M_w 7.8 Kaikōura, New Zealand, earthquake, *Bull. Seismol. Soc. Am.* **108,** no. 3B, 1496–1520.

Michael, A. J. (2012). Fundamental questions of earthquake statistics, source behavior, and the estimation of earthquake probabilities from possible foreshocks, *Bull. Seismol. Soc. Am.* **102,** no. 6, 2547–2562.

Milner, K. R., E. H. Field, W. H. Savran, M. T. Page, and T. H. Jordan (2020). Operational earthquake forecasting during the 2019 Ridgecrest, California, earthquake sequence with the UCERF3-ETAS model, *Seismol. Res. Lett.* **91,** no. 3, 1567–1578.

Milner, K. R., M. T. Page, E. H. Field, T. Parsons, G. P. Biasi, and B. E. Shaw (2013). Appendix T—Defining the inversion rupture set using plausibility filters, Uniform California Earthquake Rupture Forecast, version 3 (UCERF3), *U.S. Geol. Surv. Open-File Rept. 1165*, 14 pp.

Page, M. T., and K. Felzer (2015). Southern San Andreas fault seismicity is consistent with the Gutenberg–Richter magnitude-frequency distribution, *Bull. Seismol. Soc. Am.* **105,** no. 4, 2070–2080.

Page, M. T., E. H. Field, K. R. Milner, and P. M. Powers (2013). Appendix N—Grand inversion implementation and testing, Uniform California Earthquake Rupture Forecast, version 3 (UCERF3), *U.S. Geol. Surv. Open-File Rept. 1165*, 38 pp.

Page, M. T., E. H. Field, K. R. Milner, and P. M. Powers (2014). The UCERF3 grand inversion: Solving for the long-term rate of ruptures in a fault system, *Bull. Seismol. Soc. Am.* **104,** no. 3, 1181–1204.

Page, M. T., and N. J. van der Elst (2018). Fault-tolerant *b*-values and aftershock productivity, *J. Geophys. Res.* **123,** no. 12, 10,880–10,888.

Richards-Dinger, K., and J. H. Dieterich (2012). RSQSim earthquake simulator, *Seismol. Res. Lett.* **83,** no. 6, 983–990.

Sahakian, V., J. Bormann, N. Driscoll, A. Harding, G. Kent, and S. Wesnousky (2017). Seismic constraints on the architecture of the Newport–Inglewood/Rose Canyon fault: Implications for the length and magnitude of future earthquake ruptures, *J. Geophys. Res.* **122,** no. 3, 2085–2105.

Schwartz, D. P. (2018). Review: Past and future fault rupture lengths in seismic source characterization—The long and short of it, *Bull. Seismol. Soc. Am.* **108,** no. 5A, 2493–2520.

Shaw, B. E., K. R. Milner, E. H. Field, K. Richards-Dinger, J. J. Gilchrist, J. H. Dieterich, and T. H. Jordan (2018). A physics-based earthquake simulator replicates seismic hazard statistics across California, *Sci. Adv.* **4,** no. 8, eaau0688.

Sieh, K., L. Jones, E. Hauksson, K. Hudnut, D. Eberhart-Phillips, T. Heaton, S. Hough, K. Hutton, H. Kanamori, A. Lilje, *et al.* (1993). Near-field investigations of the Landers earthquake sequence, April to July 1992, *Science* **260,** no. 5105, 171–176.

Titus, S. J., C. DeMets, and B. Tikoff (2006). Thirty-five-year creep rates for the creeping segment of the San Andreas fault and the effects of the 2004 Parkfield earthquake: Constraints from alignment arrays, continuous Global Positioning System, and creepmeters, *Bull. Seismol. Soc. Am.* **96,** no. 4B, S250–S268.

Tong, X., D. T. Sandwell, and B. Smith-Konter (2013). High-resolution interseismic velocity data along the San Andreas fault from GPS and InSAR, *J. Geophys. Res.* **118,** no. 1, 369–389.

Wells, D. L., and B. Youngs (2013). Updated empirical relationships among magnitude, rupture area, rupture length, and surface displacement (abstract), *Seismol. Res. Lett.* **84,** no. 2, 272.

Wesnousky, S. G. (2008). Displacement and geometrical characteristics of earthquake surface ruptures: Issues and implications for seismic-hazard analysis and the process of earthquake rupture, *Bull. Seismol. Soc. Am.* **98,** 1609–1632.

Zeng, Y., and Z.-K. Shen (2014). Fault network modeling of crustal deformation in California constrained using GPS and geologic observations, *Tectonophysics* **612/613,** 1–17.

Manuscript received 12 March 2020
Published online 3 November 2020